KEK-78-25
February 1979
A

BEAM LOSS DUE TO MOMENTUM BLOW-UP IN KEK BOOSTER

Yoshikazu MIYAHARA and Tadamichi KAWAKUBO

NATIONAL LABORATORY FOR
HIGH ENERGY PHYSICS
OHO-MACHI, TSUKUBA-GUN
IBARAKI, JAPAN

KEK Reports are available from

Library
National Laboratory for High Energy Physics
Oho-machi, Tsukuba-gun
Ibaraki-ken, 300-32
JAPAN

Phone: 02986-4-1171
Telex: 3652-534 (Domestic)
(0)3652-534 (International)
Cable: KEKOHO

BEAM LOSS DUE TO MOMENTUM BLOW UP IN KEK BOOSTER

by

Yoshikazu MIYAHARA and Tadamichi KAWAKUBO

National Laboratory for High Energy Physics
Oho-machi, Tsukuba-gun, Ibaraki-ken, 300-32, Japan

Abstract

Beam intensity in the KEK booster decreases to about a half of the injected within one milli-second in the beginning of the acceleration. The mechanism of this loss is successfully explained by the momentum blow up due to the increase of the accelerating RF voltage. The loss is calculated numerically taking into account the beam distribution in the acceptance plane resulting from the multi-turn injection as well as that in the RF bucket during the acceleration. The results are in good agreement with the observations. The essential point in this calculation is that the distribution of the beam to take relatively large momentum deviation is not small but rather large because of the synchrotron motion in the RF bucket. Beam profile projected onto the horizontal plane and that to be obtained by a scraper are calculated with the use of the momentum distribution. Comparison of the calculated profiles with the observations indicates that the contribution of the momentum distribution is considerable. Finally some suggestions are made for increasing beam intensity.

§1. Introduction

In KEK booster the proton beam accumulated by the multi-turn injection method suffers serious loss within 1 msec in the beginning of the acceleration. The transmission of the beam reduces to 30 ∿ 60 % depending on the accelerating condition. It has long been a question by what process or mechanism this beam loss is induced. We show in this paper that approximately 40 % of the injected beam is lossed by the collision with septum or kicker magnet because of the shift of the equilibrium orbit due to the momentum blow-up accompanied with the increase of the accelerating RF voltage.

So far various investigations have been made in the booster to search for the reason of the beam loss. They include the study of the injection process determined by the bump and septum magnets, excitation procedure of the accelerating RF voltage, effect of the momentum spread of the injected beam, aperture or acceptance of the booster, closed orbit distoriton, effect of the leak field of the septum magnet, various resonances and space charge effects. But these contributions to the loss do not seem sufficient and the explanations with these mechanisms are not convincing because of the ambiguity of quantitative estimation. The significance of the momentum blow-up has been recognized from the first stage, but a correct estimation of the loss due to it has also been left untried. In the present paper the process of the beam loss due to the momentum blow-up is treated numerically, resulting in a quantitative agreement with the observations.

In the following we sum up a brief history of the recognition of the beam loss due to the momentum blow-up.

1) According to an adiabatic capture, the injected beam can be captured in the RF bucket up to 96 %[1)]
2) Aperture of the booster ring is ±50 mm, determined by the septum and kicker magnets. Closed orbit distortion is about ±5 mm. The momentum spread $\Delta p/p$ of the beam reaches to the maximum ±1 % around 1 msec after injection, introducing the maximum shift of the equilibrium orbit $\Delta R = X_p \cdot \Delta p/p \approx \pm 14$ mm, where X_p is the momentum dispersion function. Therefore the transmission of the beam up to 1 msec is T = (50-5-14)/(50-5) = 69 %.

3) The beam rotates in the x-x' plane because of the betatron oscillation. If we assume a uniform distribution in the plane the transmission is reduced squarely to 47 %.

4) Since the momentum distribution is smaller in regard to the beam with larger deviation, the transmission above obtained is over-estimation. This consideration leads to the transmission of 75 ∿ 80 %.[2)]

However, we had a doubt about the last estimation. The beam injected in the RF bucket rotates in the bucket owing to the synchrotron motion, so that the ratio of the beam to take a larger momentum deviation is not small as is expected from, for example, a Gaussian distribution but rather large. According to this idea we have calculated in detail the transmission of the beam up to 1 msec and obtained the value ∿60 %, in a satisfactory agreement with the observed value.

Following calculation of the beam loss requires the knowledge of the distribution of the injected beam in the x-x' plane, which is obtained by the calculation of the multi-turn injection process. The result is presented in section 2. Next the beam transmission is calculated taking into account the momentum blow-up, where the results is compared with the observations. Then we calculate the beam profiles utilizing the data of the beam distribution in the x-x' plane and in the RF bucket, and compare them with the profiles observed with the use of a scraper and a non destructive profile monitor. Finally a way to increase the beam intensity is considered taking into account the above results.

§2. Beam distribution in the x-x' plane

The proton beam with the energy 20 MeV and the current 100 mA is transported from a linac and injected into the booster by the multi-turn injection method. The emittance of the injected beam is $67\ \pi \times 10^{-6}$ rad·m where 100 % of the beam are contained. The beam distribution in the x-x' plane after the multi-turn injection process was calculated, as depicted in Fig.1. The acceptance drawn by the outer ellipse in the figure is $A = 710\ \pi \times 10^{-6}$ rad·m. At 50 mm apart from the center beam line there locates the septum of the septum magnet, which determines the

aperture W of the booster. The aperture of the kicker magnet for beam extraction is also ±50 mm.

As will be understood later it is necessary to get the beam distribution in restricted acceptance A_r. According to the betatron oscillation the beam rotates in the x-x' plane along the trajectories shown in Fig.1. By counting the area of the injected beam in each trajectory shell and accumulating them we get an approximate beam distirbution in the restricted acceptances as shown in Fig.2-a, where the abscissa x_A is related to $A_r = (x_A/W)^2 A$. The figure (a) displays a square distribution as expected first. This figure is, however, obtained on the assumption that the beam distribution is uniform in the whole emittance of the injected beam. We should note that really the beam is more concentrated in the central region of the emittance or 80 % of the injected beam is measured to be within the emittance $\varepsilon = 22\pi \times 10^{-6}$ rad•m. Although it is possible to calculate accurately the beam distribution in the restricted acceptances by taking into account the detailed distribution in the emittance plane, we assume in the following a uniform distribution only within the emittance $22\pi \times 10^{-6}$ rad•m because of simplicity and intuitive understanding. Figure 3 shows the distribution of the injected beam with the emittance $\varepsilon = 22\pi \times 10^{-6}$ rad•m, which is picked out of Fig.1. We know from the figure that the beam distribution is rather separated and weak on the average, thus being open to a further increase of the beam intensity as described later. Figure 2-b represents the beam distribution in the restricted acceptances for this case, similarly obtained as before. The distribution follow the linear relation

$$y = \alpha\, x_A\ (\text{mm}) - \beta \qquad (1)$$

where $\alpha = 2.56$ and $\beta = 28.2$. This linearity results from the fact that the beam is injected separately and spirally with a constant angle $\sim\pi/3$ in the x-x' plane. The angle is related to the decimal part of the betatron oscillation number $\nu = 2.17$. We will use in the next section the linear relation for the calculation of the beam loss due to the momentum blow up. As seen from Figs.1~3, the beam is now not injected in the central region of the x-x' plane, the hole radius being $h \approx 11$ mm, which will be discussed later again.

§3. Beam distribution in the RF bucket

In order to calculate the beam loss it is further necessary to know the momentum distribution of the injected beam in the RF bucket; how the beam is injected into the RF bucket and how the bucket structure changes in accompanying with the RF acceleration. The momentum distribution is different day by day and on the average we may assume a triangular distribution as shown with σ_L in Fig.4-a, there the maximum momentum deviation being ±0.48 %. The height of the RF bucket awaiting the beam is given by,[3]

$$\left(\frac{\Delta p}{p}\right)_e = \pm\frac{1}{\beta}\sqrt{\frac{eV}{\pi h\eta E}\left[(\pi - 2\phi_s)\sin\phi_s - 2\cos\phi_s\right]} \qquad (2)$$

where β is the velocity divided by the light velocity, e the unit charge, V the RF voltage, h the harmonic number, $\eta = \alpha - \frac{1}{\gamma^2}$, α the momentum compaction factor, γ the relativistic energy, E the total energy and ϕ_s the phase angle for the synchronous particle. For the ordinary operation of the RF voltage V (t=0) = 1.3 kV and $\phi_s = 180°$, we get $(\Delta p/p)_e = \pm 0.52$ %. This is nearly equal to the momentum spread of the injected beam. On this condition the beam is more stable longitudinally during the acceleration.[4]

The injected beam rotates in the RF bucket by the synchrotron motion and draws trajectries according to the following equation,[3]

$$\left(\frac{\dot{\phi}}{\Omega_s}\right)^2 - \frac{1}{\cos\phi_s}(\cos\phi + \sin\phi_s) = \text{const} \leq 2 \qquad (3)$$

where ϕ is the phase angle and Ω_s is the synchrotron oscillation frequency. We divide the bucket into several regions (X = A ∿ J) along the trajectories. A quarter of the bucket is shown in Fig.4-b. Note that $\dot{\phi}/\Omega_s$ is proportional to $\Delta p/p$.

The trajectory shells are further divided into small areas as shown in the figure. Particle number injected in the small area is proportional to the product of the area a and the corresponding momentum distribution σ_L of the injected beam. Taking into account the synchrotron motion we sum the particle number in the trajectory shells. Figure 4-c indicates the sum σ_x for each shell x = A,B,C···,where $(\Delta p/p)_x$ is the maximum momentum deviation in the trajectory shells. About 24 % of the beam are

injected outside the bucket denoted by K. An important point is that more particles are injected in the outer shell as expected at first, which is contrary to the assumption made in the calculation in the reference 2). The shaded distribution in Fig.4-c is the resultant at 1 msec having suffered the beam loss as described in the following.

The synchronous phase makes shift according to the relation

$$\sin\phi_s = \frac{2\pi R\rho}{V(t)}\,\omega B_{AC}\,\sin\omega t \qquad (4)$$

where R is the mean radius, ρ the curvature, $B_{AC}\sin\omega t$ the AC field due to a sinusoidal current with the frequency $\omega/2\pi$. Accompanied with the increase of the acceleration voltage, the bucket height also increases, taking the maximum value around 1 msec after injection $(\frac{\Delta p}{p})_{max} = 1.23$ % for the voltage V(1 msec) = 9.0 kV as shown in Fig.5. The bucket area A_{RF} and the synchronous phase ϕ_s are also shown in the figure. Although the bucket spread shrinks from 0 ∿ 360° at injection to 8 ∿ 298° at 1 msec as shown in Figs.4-b and 6-a, these bucket shapes are not so much different, therefore we assume that the beam injected into a given trajectory shell keeps to belong to the same or corresponding shell so long as 1 msec. The synchrotron frequency in the linear region is given by[3)]

$$\Omega_s = \frac{\omega_0}{\beta}\sqrt{\frac{\eta\cos\phi_s}{2\pi}\frac{eV}{E}} \qquad (5)$$

where $\omega_0/2\pi$ is the revolution frequency. At t = 0 and 1 ms, $\Omega_s/2\pi$ = 3.1 and 8.3 kHz, respectively, therefore the beam rotates several times in the RF bucket until 1 msec. Of course the betatron oscillation is very fast (∿ 4 MHz) and the beam rotates many many times in the x-x' plane.

§4. Calculation of the beam loss

It is ready now to calculate the beam loss due to the momentum blow-up. In the preceding section we have shown that the beam number contained in the restricted acceptance is given by the equation (1). The beam injected with the momentum deviation $(\Delta p/p)_1$ takes an equilibrium orbit ΔR_1 $(= X_p\,(\Delta p/p)_1)$, and the effective aparture is $W - \Delta R_1$. Thus the number of such a beam is $n_1 = k\{\alpha(W - \Delta R_1) - \beta\}$ where k is a constant.

In the course of the rotation along the trajectory shell, the beam takes several times until 1 msec the maximum momentum deviation $(\Delta p/p)_x$ associated to the shell, then the beam number is reduced to $n_2 = k\{\alpha(W - \Delta R_x) - \beta\}$. The number of the particles, which are injected into the small area a in the RF bucket (Fig.4-b) with the momentum distribution σ_L, is also proportional to $a\sigma_L$. Therefore the number of the particles transmitted up to 1 msec is given by

$$n_2 = k' \frac{\{\alpha(W - \Delta R_x) - \beta\}}{\{\alpha(W - \Delta R_1) - \beta\}} a\sigma_L . \qquad (6)$$

This calculation was made for every small area in Fig.4-b. Thus the total transmission of the beam injected into the bucket up to 1 msec is given by

$$T_B = \frac{\Sigma n_2}{\Sigma n_1} = 73\ \% . \qquad (7)$$

Since only 76 % of all the beams are injected into the bucket as seen from Fig.4-c, the over-all transmission is $T_0 = 55$ % for the aperture W = 50 mm.

The beam loss calculation described above corresponds to such a case that the bucket height increases very slowly since we have assumed that the beam injected outside the bucket is not captured into the bucket in the course of the acceleration. In reality some beams injected outside the bucket are also captured because of the rather rapid increase of the bucket height (adiabatic capture). A simulation of this capture process indicates a 96 % capture of the injected beam.[1] In an attempt to measure the capture efficiency a thin beam experiment has been made by injecting a chopped beam which is 1 μsec long while the period of the revolution in the booster ring is 0.62 μsec. Figure 7 shows the experimental transmission and size- and-position of the beam as a function of the injection timing from the peak of the bump decay field. The figure indicates that the RF capture efficiency is more than 80 % for the beam injected in the center of the vacuum chamber, no loss being expected for such a beam due to the momentum blow-up.

The other extreme case is that the bucket height at injection is

the same with that at 1 msec because of very rapid increase. The beam distribution for this case is obtained similarly and represented in Fig.8. The probability of the beam injected in the bucket is 90 %, the transmission with respect to the beam in the bucket is 76 %, therefore the over-all transmission results in 68 %. Table 1 summarizes the results for the aperture W = 50 mm as well as for W = 40 mm. Because of the closed orbit distortion ±5 mm the effective aperture is W ≈ 45 mm, thus the over-all transmission is concluded to be around 60 %.

Table 1 Calculated transmission of the beam

Increse of bucket height	slow		rapid	
Aperture W (mm)	50	40	50	40
Prob. in bucket (%)	76	76	90	90
Transmission in bucket T_B (%)	73	63	76	67
Over all transmission T_0 (%)	55	48	68	60

Figure 9-a represents the beam intensity of the booster from the injection to the extraction, which indicates a rapid decrease of the beam until 1 msec. Figure 9-b shows the beam intensity with fast and slow response monitors in the beginning of the acceleration. Note the wavy structure of the slow intensity monitor, which is associated with the build-up of the filamentation as seen with the fast intensity monitor. The periods of these waves are 75 μsec and agree with a quarter of the synchrotron oscillation period. This wavy structure of the slow intensity monitor indicates that the beam is mainly lossed with the shift of the equilibrium orbit and supports the loss mechanism described above.

§5. Beam profile by a scraper

In this section is considered what profile of the beam will be obtained when a scraper is inserted little by little toward the center of the vacuum chamber, and this is compared with the experimental observation. Since the scraper is a mechanical cutter of the beam it pro-

vides a surer picture of the beam profile than the other profile monitor. But the picture obtained by the scraper does not straightforwardly give the distribution in the x-x' plane and should be taken carefully since the contribution of the momentum distribution is considerable as described as follows. Experimentally the beam intensity at 1 msec after injection was measured as a function of the horizontal position of the scraper edge, which is shown in Fig.2-d.

As described in §2 the particle number contained in the restricted acceptance is given by the equation (1), which means a constant beam distribution per unit length Δx_A in the range from h (= 11 mm) to W (aperture). Taking account of a momentum distribution $\sigma(\Delta p/p)$, the particle number contained in $0 \sim x_A$, which is the intensity not cut off by the scraper, is calculated by

$$F(x_A) = \sum_{\Delta p/p} k\sigma \{x_A - (\Delta R + h)\} \qquad (8)$$

where k is a constant and $\Delta R = X_p \Delta p/p$. As for σ we should take the beam distribution σ_x(1 msec) of the trajectory shell shown in Fig.4-c since until 1 msec the synchrotron oscillation elapses several times and the bucket height increases monotonically. The result of the calculation is shown in Fig.2-c for the case of the slow increase of the bucket height. The agreement between (c) and (d) is good when we take into account that (c) is obtained for the aperture W = 50 mm but the real aperture is ∿45 mm because of the closed orbit distortion. Thus the point P is only needed to move to the point Q in the figure.

§6. Beam profile projected on the horizontal plane

Adding to the scraper experiment, we can obtain the information of the beam from a non-destructive profile monitor. This measures the beam distribution in the real space by gathering the charged gas being ionized by the circulating beam.[5] It provides the projected profile of the beam distribution in the x-x' plane onto the horizontal plane. We calculate the horizontal profile taking into account the momentum distribution as well as the distribution in the x-x' plane and compare it with the observation. The profile was measured at 1 msec after injection within a few tens μsec , much shorter than the synchrotron oscillation period

but much longer than the betatron oscillation period.

The momentum distribution is almost the same during the measurement and given by σ_T in Fig.6-b, which is the projection of the distribution in the bucket onto the $\Delta p/p$ axis. The distribution in the bucket is obtained by distributing uniformly the resultant distribution at 1 msec, as obtained in §4 in regard to Fig.4-b, into the corresponding trajectory shell of Fig.6-a.

Although the acceptance of the x-x' plane is an ellipse we may reduce it to a circle with the condition that the beam distribution is constant in each trajectory shell. The particles rotate along the trajectory shell about one hundred times with a step $2\pi\nu_x$ during the measurement in regard to a given point of the booster ring. Each particle has the probability to find itself about once everywhere in a bit angle $\sim 3.6°$ along the trajectory shell. Therefore each particle has the same probability ($\sim$once) to kick and ionize the gas in the region $x \sim x+\Delta x$. As described above, every shell contains almost the same number of particles. Therefore the non-destructive profile is obtained by counting the area of the circle in the region $x \sim x+\Delta x$ with the condition that the beam distribution is constant in the circle.

With the use of the notations in Fig.10, the small shaded area is given by

$$\Delta a = \frac{r}{\cos\theta}\,\Delta\theta\Delta x. \tag{9}$$

The charged gas distribution in $x \sim x+\Delta x$ is given by

$$n(x) \propto \int_0^{\theta_1} \Delta a$$

$$= \Delta x \cdot x\tan\theta_1 \quad , \tag{10}$$

where $R\cos\theta_1 = x$. Taking into account the hole of the distribution in the x-x' plane, we subtract n'(x) from n(x),

$$n'(x) \propto \Delta x \cdot x\tan\theta_2$$

$$h\cos\theta_2 = x \quad , \tag{11}$$

where h is the hole radius. When we take into account the momentum distribution, we set $R = W - \Delta R(\Delta p/p)$, replace x by $x - \Delta R(\Delta p/p)$ and get the profile by the relation,

$$N(x) \propto \sum_{-\Delta p_{max}}^{+\Delta p_{max}} [n(x) - n'(x)]\sigma_T(\Delta p/p). \qquad (12)$$

These calculations were made numerically and the results are shown in Fig.11, which are compared with the observation (Fig.11-e). Rather deep bump of the profile due to the hole is saved by the consideration of the momentum distribution. Although the agreement with the observation is not so good, the figures indicate that the consideration of the momentum distirbution is necessary to understand the non-destructive profile correctly.

§7. For the increase of the beam intensity

As seen from Fig.1, the beam injected by the multi-turn injection process distributes fully to the limit of the aperture W = ±50 mm. The aperture is now determined by the aperture of the septum and kicker magnets. The closed orbit distortion is about ±5 mm. The average shift of the equilibrium orbit due to the momentum deviation is about 10 mm. Therefore effective aperture x_A is about ±35 mm. The acceptance at injection is $710\pi \times 10^{-6}$ rad·m and the effective acceptance is $350\pi \times 10^{-6}$ rad·m. By the adiabatic damping of the factor $B_{min}/B_{max} = 1/5.5$, the emittance of the extracted beam should be $63\pi \times 10^{-6}$ rad·m. This is in accord with the measured value $50 \sim 60\pi \times 10^{-6}$ rad·m.[6] Therefore only the beam injected in the effective acceptance $350\pi \times 10^{-6}$ rad·m is transmitted and accelerated up to 25 msec.

In order to increase the beam intensity following improvements will be fruitful;

1. increase of the aperture (especially of the septum and kicker magnets),
2. correction of the closed orbit distortion,
3. possible suppression of the RF bucket height,
4. increase of the brightness of the transported beam from the linac,

5. increase of the multi-turn injection efficiency.

The increase of the effective aperture by ±5 mm will bring about the increase of the beam intensity by ∿20 %, which is inferred from the intensity dependence on the scraper edge in Fig.2-d. The average density in the acceptance plane is at present weak as seen in Fig.3. The beam is injected separately and not injected in the central region. The beam distribution in the plane can be made more dense or compact by lengthening the decay time of the bump magnet field and drawing the ν value near the integer.

§8. Conclusion

As described above we have succeeded in explaining quantitatively the beam loss until 1 msec from injection by the mechanism of the shift of the equilibrium orbit due to the momentum blow-up. The essential point is that the distribution of the beam to take a larger momentum deviation is not small but rather large because of the synchrotron motion in the RF bucket. This fact also contributes considerably to the beam profiles which are obtained with the scraper or by the non-destructive profile monitor. The profiles are not simply the projections of the beam distribution in the x-x' plane, but affected much by the momentum distribution. Now it is clear that in order to save the beam loss until 1 msec it is necessary to make wide the aperture determined by the kicker and septum magnets or to correct the closed orbit distortion. Another way to improve the beam intensity is to make the beam from the injector more intense or to improve the efficiency of the multi-turn injection, which seems very promising as inferred from Fig.3.

Acknowledgement

The authors are grateful to Professors E. Ezura, Y. Kimura, M. Kondoh and H. Sasaki for valuable discussions.

References

1) M. Kondoh et al.: KEK Annual Rept. (1972) 60.
2) E. Ezura: private communication.
3) H. Bruck: Accélérateurs Circulaires de Particules (Presses Universitaires de France, 1966) Chap. 4.

4) E. Ezura and S. Takeda: KEK - ASN-81 (1977)

5) H. Ishimaru, Z. Igarashi, M. Muto and S. Shibata: Particle Accelerator Conference, Chicago (1977) 1821.

6) KEK Annual Rept. (1975) 55.

Figure caption

Fig.1 Distribution of the beam injected by the multi-turn injection. The emittance of the injected beam is $67\pi \times 10^{-6}$ rad·m and the acceptance of the booster is $711\pi \times 10^{-6}$ rad·m.

Fig.2 Beam distribution in the restricted acceptance. The symbols (o) and (•) denote the distribution obtained from Fig.1 and Fig.3 respectively. The equations in the figures are the best fit. The symbol (Δ) represents the beam intensity not cut off by the scraper, being calculated in §5, which should be compared with the observation (d).

Fig.3 Beam distribution picked out of Fig.1. The emittance of injected beam is now restricted to $22\pi \times 10^{-6}$ rad·m, where 80 % of the beam is contained.

Fig.4 The averaged momentum distribution σ_L of the beam from the linac (a), a quarter of the RF bucket (b), which is divided to ten trajectory shells A, B, ··· J, and the beam distribution σ_x in each trajectory shell and outisde the bucket at t=0 and 1 msec (c).

Fig.5 Accelerating RF voltage V, maximum momentum deviation $(\Delta p/p)_e$, bucket area A_{RF} synchrotron oscillation frequency $\Omega_s/2\pi$ and synchronous phase ϕ_s during the acceleration.

Fig.6 RF bucket at 1 msec after injection (a). The figure (b) represents the beam distribution σ_T projected onto the $\Delta p/p$ axis as explained in §6.

Fig.7 Experimental beam transmission I (1 msec)/I_0 of the chopped beam with 1 μsec long (a) and the beam size-and-position of the first half turn (b). The abscissa is the injection timing from the peak of the decaying bump field.

Fig.8 Beam distribution similar to Fig.4. The bucket height is assumed to be $\Delta p/p = 1.23$ % in the range $t = 0 \sim 1$ msec.

Fig.9 Beam intensity from injection to ejection (a), and those around injection (b) with fast and slow intensity monitors.

Fig.10 Notations in the acceptance plane.

Fig.11 Beam profiles projected on the horizontal plane.

	a	b	c	d
hole	x	o	x	o
momentum distribution	x	x	o	o

(e) is the observed profile at 1 msec.

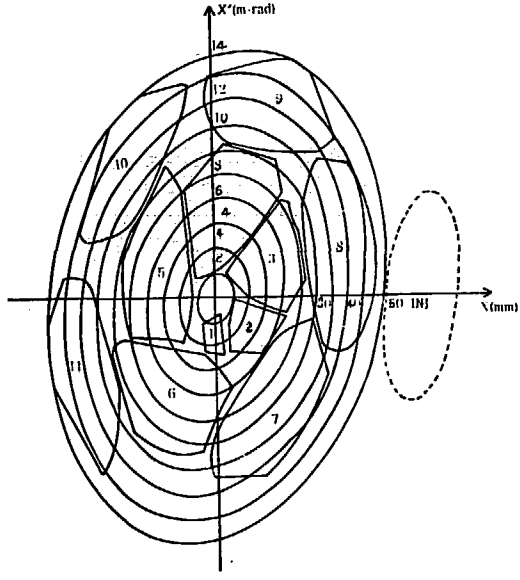
X'(m·rad)
(mm)

Fig.1

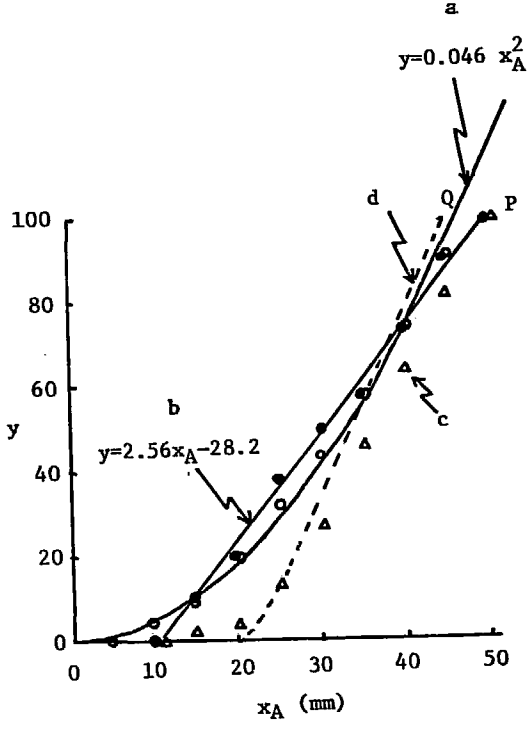
a
y=0.046 x_A^2
d
Q
P
100
80
60
y
b
y=2.56x_A-28.2
40
20
0
c
0
10
20
30
40
50
x_A (mm)

Fig.2

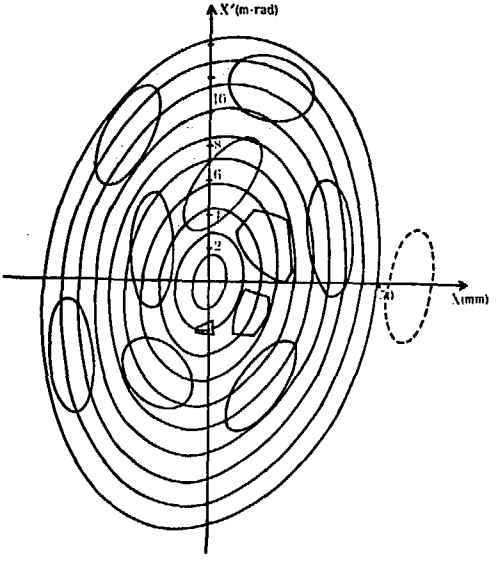
X'(m-rad)
10
8
6
4
2
X(mm)

Fig.3

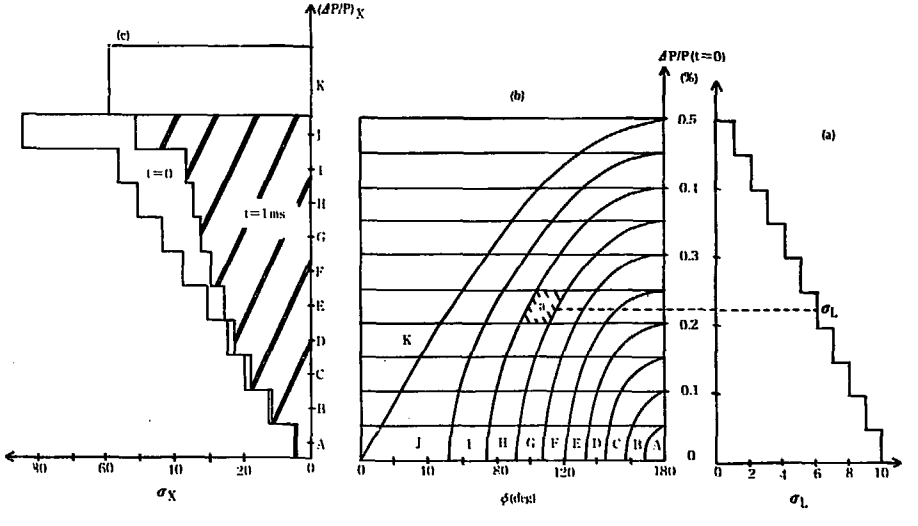
(c)
(ΔP/P)X
K
J
I
H
G
F
E
D
C
B
A
t=0
t=1ms
90
60
10
20
0
σX
(b)
ΔP/P(t=0)
(%)
0.5
0.1
0.3
0.2
0.1
0
K
J
I
H
G
F
E
D
C
B
A
0
10
80
120
180
φ(deg)
(a)
σL
0
2
4
6
8
10
σL

Fig.4

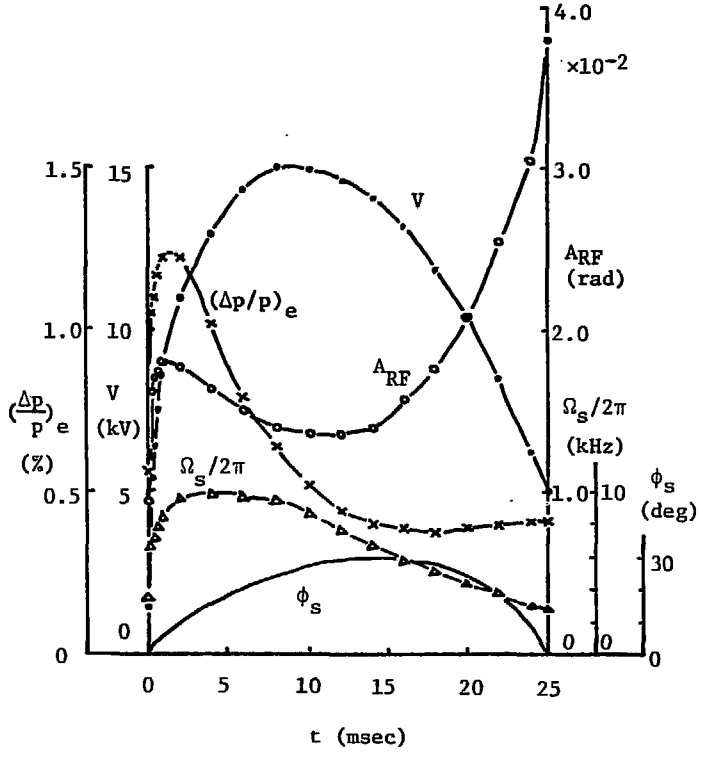
4.0
×10⁻²
1.5
15
3.0
V
A_RF
(rad)
(Δp/p)e
1.0
10
2.0
A_RF
V
(kV)
Ω_s/2π
(kHz)
(Δp/p)e
(%)
Ω_s/2π
0.5
5
1.0
10
φ_s
(deg)
30
φ_s
0
0
0
0
0
5
10
15
20
25
t (msec)

Fig.5

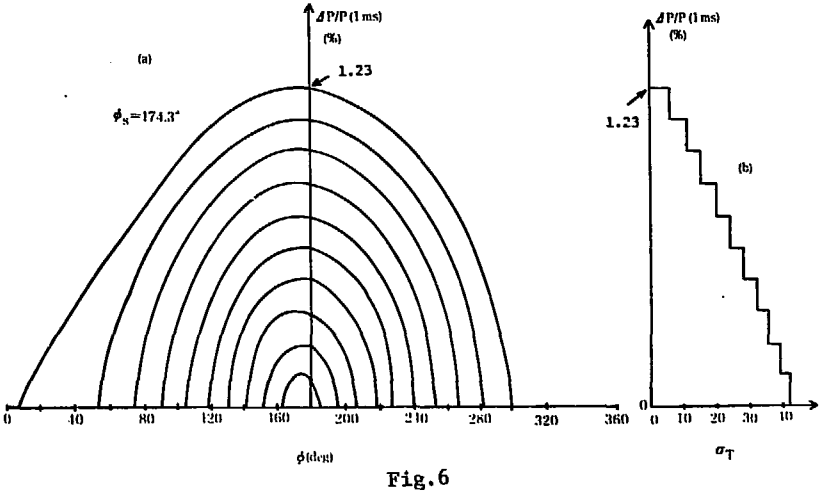
ΔP/P (1 ms)
(%)
(a)
1.23
φ_s=174.3°
0
40
80
120
160
200
240
280
320
360
φ(deg)
ΔP/P (1 ms)
(%)
1.23
(b)
0
0
10
20
30
40
σ_T

Fig.6

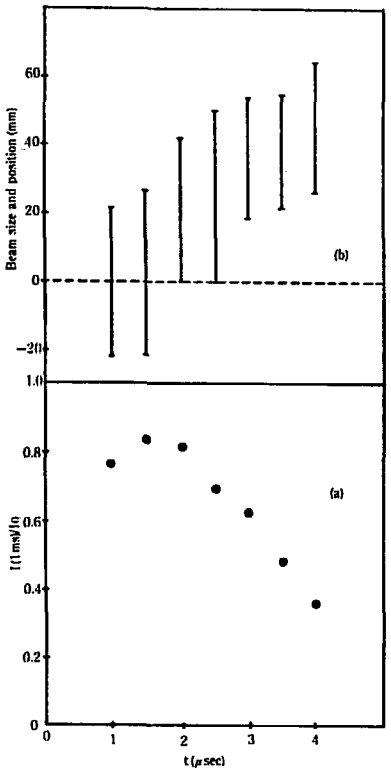
Beam size and position (mm)
60
40
20
0
-20
(b)
1.0
0.8
0.6
0.4
0.2
0
I(1 ms)/I0
(a)
0
1
2
3
4
t (μsec)

Fig.7

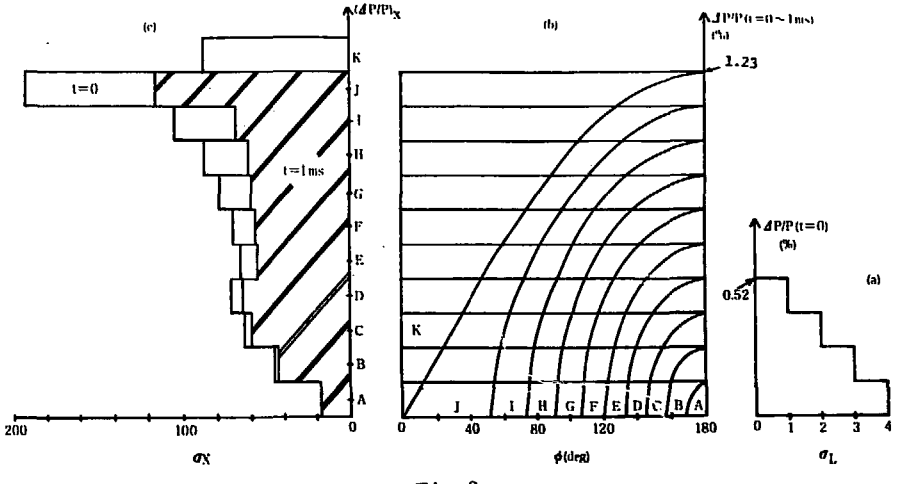
(c)
ΔP/P)x
t=0
t=1ms
K
J
I
H
G
F
E
D
C
B
A
200
100
0
σx
(b)
ΔP/P(t=0~1ms)
(%)
1.23
K
J
I
H
G
F
E
D
C
B
A
0
40
80
120
180
φ(deg)
ΔP/P(t=0)
(%)
(a)
0.52
0
1
2
3
4
σL

Fig.8

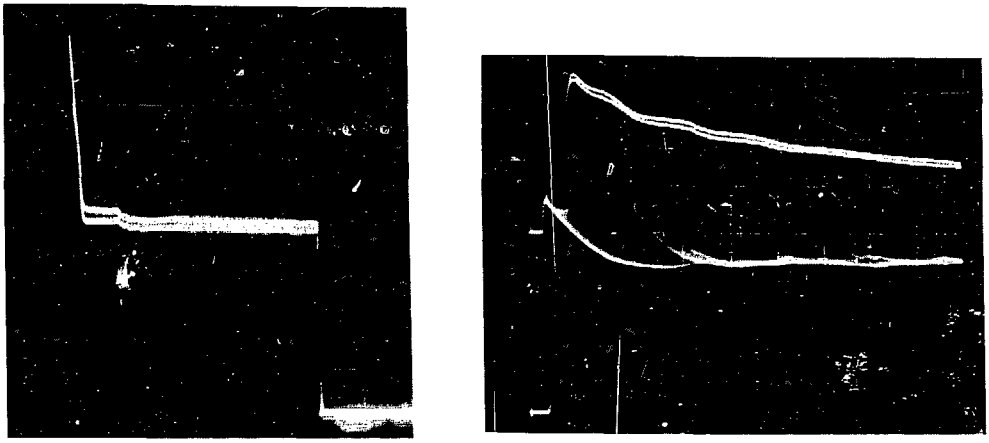

a b

Fig.9

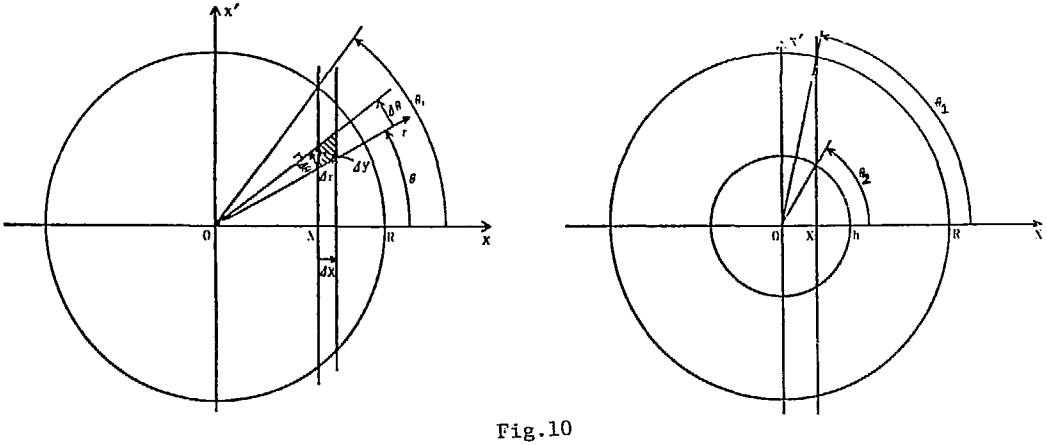

Fig.10

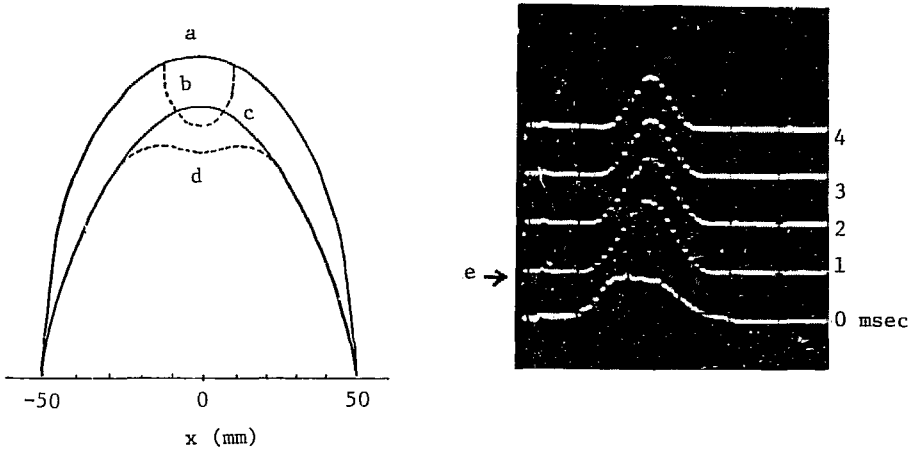

Fig.11